npj | science of food

Article

Published in partnership with Beijing Technology and Business University & International Union of Food Science and Technology

https://doi.org/10.1038/s41538-025-00453-4

Compartmentalization of heme biosynthetic pathways into yeast mitochondria enhances heme production

Check for updates

Jae Yoon Won[1,2,4], Hyun-Jae Lee[1,2,4], Eun Bi Yoon[1,2], Young-Wook Chin[3] ✉ & Sun-Ki Kim[1,2] ✉

Saccharomyces cerevisiae is a generally recognized as safe (GRAS) workhorse strain widely used in the food industry for the cost-effective production of food ingredients. However, the heme production yield in yeast is significantly lower than in bacteria for two main reasons: (1) the heme biosynthetic pathway is bifurcated into the cytosol and mitochondria, and (2) yeast's heme biosynthetic protoporphyrin-dependent (PPD) pathway is thermodynamically unfavorable compared with bacteria's coproporphyrin-dependent (CPD) pathway. To overcome these limitations, the PPD and CPD pathways were compartmentalized into the mitochondria by attaching mitochondria-targeting sequences (MTSs) to the N-terminus of the enzymes. All the enzyme activities required for the CPD pathway are present in *S. cerevisiae*, except for copro-heme decarboxylase (HemQ); therefore, bacterial HemQ with the N-terminal MTS was introduced to complete the CPD pathway. The resulting *S. cerevisiae* H4+$_{MTS9}$HemQ^{Cg} strain with mitochondrial PPD and CPD pathways showed 65% higher heme concentration than the engineered strain with only the mitochondrial PPD pathway. Furthermore, the functional expression level of HemQ from *Corynebacterium glutamicum* was significantly enhanced in vitro and in vivo by the co-expression of Group-I HSP60 chaperonins (GroEL and GroES) derived from *Escherichia coli*. The engineered *S. cerevisiae* H4+$_{MTS9}$HemQ^{Cg}+GroELS strain containing the mitochondrial PPD and CPD pathways and the Group-I HSP60 chaperonins produced the highest heme concentration (4.6 mg/L), which was 17% higher than that produced by the H4+$_{MTS9}$HemQ^{Cg} strain.

Heme is a porphyrin/iron complex cofactor, ubiquitous in microorganisms, plants, and animals[1], which is important to aerobic life. Heme has several biological functions, including oxygen transport, electron transfer, energy production, and protection from oxidative damage[2,3]. Furthermore, heme is of interest in a variety of applications, including as a medical treatment for iron deficiency and acute intermittent porphyria[4], a natural pigment in food coloring to replace carcinogenic synthetic pigments[5], a precursor to porphyrin derivatives used in disease diagnosis and treatment[6], and a charge enhancer for lithium batteries[7]. Recently, heme has received attention in the artificial meat industry as a key ingredient to mimic the flavor of meat[8].

Heme is primarily obtained by extraction from animal blood, which has resulted in significant concerns, such as animal welfare and environmental pollution from organic solvents used in the extraction process[9]. Therefore, developing microbial cell factories to produce heme using biotechnology is crucial for its sustainable and economical production. To date, *Escherichia coli*, *Corynebacterium glutamicum*, *Bacillus subtilis*, *Pichia pastoris*, and *Saccharomyces cerevisiae* have been engineered to produce heme. Choi et al.[10] reported that engineered *E. coli* produced the highest concentration of heme (1.03 g/L) with a yield of 4.14 mg of heme/g of glycerol in a fed-batch fermentation; however, the endotoxin secreted by *E. coli* is a safety concern, especially if this system were used in the food industry[11]. In contrast, the highest titer of heme produced in fed-batch fermentation with *S. cerevisiae*, a generally recognized as safe (GRAS) host often used to produce food ingredients, was found to be 380.5 mg/L[12]. In particular, yeast extracts with a high heme content are often used as color and flavor enhancers in plant-based meat alternatives[13]. Therefore, this study aimed to develop a novel strategy to improve heme production in *S. cerevisiae*.

[1]Department of Food Science and Technology, Chung-Ang University, Anseong, Gyeonggi, Republic of Korea. [2]GreenTech-based Food Safety Research Group, BK21 Four, Chung-Ang University, Anseong, Gyeonggi, Republic of Korea. [3]Research Group of Traditional Food, Korea Food Research Institute, Wanju, Republic of Korea. [4]These authors contributed equally: Jae Yoon Won, Hyun-Jae Lee. ✉e-mail: ywchin@kfri.re.kr; skkim18@cau.ac.kr

The mitochondria of *S. cerevisiae* produce 5-aminolevulinic acid (ALA), a common porphyrin precursor, from glycine and succinyl-coenzyme A via the C4 pathway[14]. After ALA is transported into the cytoplasm, it is converted to coproporphyrinogen III or protoporphyrinogen IX in a cascading reaction catalyzed by four or five enzymes (Fig. 1A). Whether ALA is converted to coproporphyrinogen III or protoporphyrinogen IX in the cytoplasm is determined by the location of coproporphyrinogen III oxidase (HEM13). Some authors have reported that HEM13 is present in yeast cytoplasm[15,16], while others have reported that it is present in the mitochondria, forming a complex with protoporphyrinogen/coproporphyrinogen III oxidase (HEM14) and protoporphyrin/coproporphyrin ferrochelatase (HEM15)[17,18]. In *S. cerevisiae* the bifurcation of the heme biosynthetic pathway reduces the efficiency of heme production because the intermediates must be transported across the mitochondrial membranes[15]. To overcome this limitation, we aimed to compartmentalize the entire heme biosynthesis pathway into the mitochondria (Fig. 1B).

Heme is synthesized from uroporphyrinogen III via three distinct pathways depending on the species: the protoporphyrin-dependent (PPD), coproporphyrin-dependent (CPD), and siroheme-dependent pathways[19,20]. Although the PPD pathway exists for heme synthesis in *S. cerevisiae*, it is thermodynamically unfavorable compared to the CPD pathway, a recently discovered non-canonical pathway present in Firmicutes and Actinobacteria. Indeed, the $\Delta G^{0\prime}$ value for the entire reaction in the CPD pathway is 447.22 kJ/mol lower than the corresponding value in the PPD pathway[21]. Therefore, we decided to utilize the PPD and CPD pathways for efficient production of heme in *S. cerevisiae*. The PPD and CPD pathways are identical up to the synthesis of coproporphyrinogen III but differ in the subsequent heme production steps (Fig. 1B). In the CPD pathway, heme is produced from coproporphyrinogen III through three consecutive reactions catalyzed by HEM14, HEM15, and copro-heme decarboxylase (HemQ). However, HemQ is not present in *S. cerevisiae*; therefore, we introduced HemQ from Gram-positive bacteria to complete the CPD pathway. The

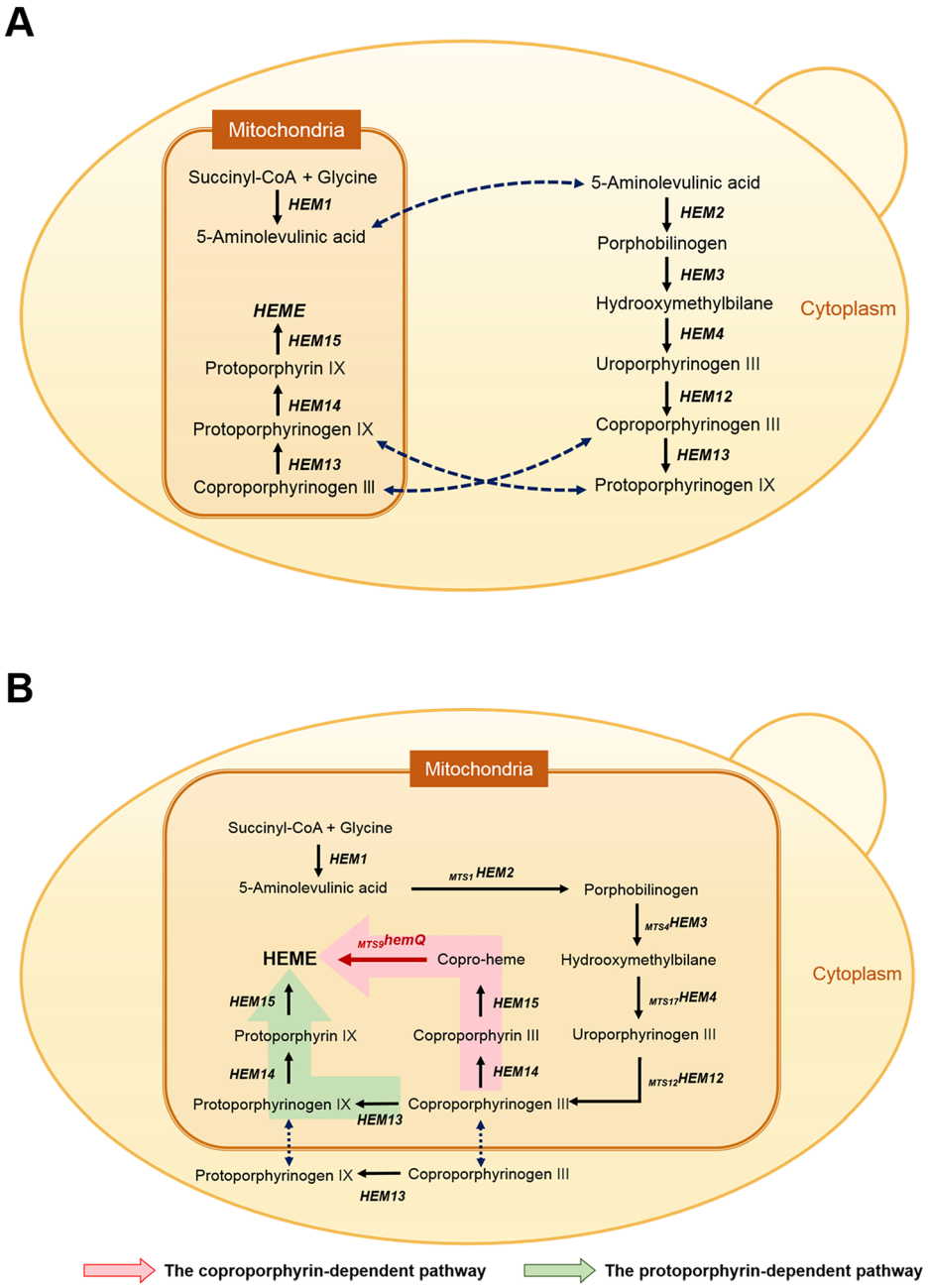

Fig. 1 | Target pathways and overall engineering strategies for efficient heme synthesis. A In wild-type *Saccharomyces cerevisiae*, the heme biosynthetic pathway is bifurcated between the cytoplasm and mitochondria. Blue arrows depict transport across mitochondrial membranes. **B** In engineered *S. cerevisiae*, heme was synthesized via the protoporphyrin-dependent and coproporphyrin-dependent pathways. The coproporphyrin-dependent pathway, which is not present in the wild type, was completed by introducing HemQ from Gram-positive bacteria. In addition, the complete pathways were targeted to mitochondria by attaching mitochondria targeting sequences (MTSs) at the N-terminus of HEM2, HEM3, HEM4, HEM12, and HemQ.

CPD pathway was also compartmentalized into mitochondria by attaching a mitochondria-targeting sequence (MTS) to HemQ (Fig. 1B).

Results and discussion

Effects of mitochondrial compartmentalization of the protoporphyrin-dependent pathway on *S. cerevisiae*'s heme production

The translocation of mitochondrial proteins into the mitochondria is mediated by the MTSs present at the N-terminus of the mitochondrial proteins. Accordingly, MTSs were attached to the N-termini of HEM2, porphobilinogen deaminase (HEM3), uroporphyrinogen III synthase (HEM4), and HEM12 to translocate them into the mitochondria. Since using the same type of MTS could result in the removal of the recombinant genes by homologous recombination, different types of MTSs were attached to the N-termini of HEM2, HEM3, HEM4, and HEM12 as follows: $_{MTS1}$HEM2, HEM2 with N-terminal MTS1 derived from MMF1 (mitochondrial matrix protein); $_{MTS4}$HEM3, HEM3 with N-terminal MTS4 derived from yeast mitochondrial chaperonin 60 (HSP60); $_{MTS17}$HEM4, HEM4 with N-terminal MTS17 derived from zinc binding subunit of cytochrome c oxidase (COX4); $_{MTS12}$HEM12, HEM12 with N-terminal MTS12 derived from lipoamide dehydrogenase (LPD1). A previous study found that the preceding set of MTSs could be utilized to compartmentalize multigene biosynthetic pathways into *S. cerevisiae* mitochondria[22]. The genes encoding $_{MTS1}$HEM2, $_{MTS4}$HEM3, $_{MTS17}$HEM4, and $_{MTS12}$HEM12 were expressed under the transcriptional control of a strong constitutive glyceraldehyde-3-phosphate dehydrogenase (GPD) promoter to construct the Mito-H4 strain. The Cyto-H4 strain expressing HEM2, HEM3, HEM4, and HEM12 without MTSs under the transcriptional control of the GPD promoter was constructed as a control.

To ensure the mitochondrial compartmentalization of the enzyme via MTS attachment, the mitochondria were fractionated from the control *S. cerevisiae* D452-2 and recombinant strains expressing $_{MTS1}$HEM2 and HEM2 with a C-terminal Myc-tag. Western blot analysis of the mitochondrial fractions using anti-Myc antibody showed that the HEM2 protein was only present in the Mito-H4 strain's mitochondria (Supplementary Fig. 1). This result suggested that HEM2 was successfully relocalized to the mitochondria by attaching MTS to its N-terminus. In the batch fermentations, the *S. cerevisiae* wild-type D452-2, Cyto-H4 (amplified cytoplasmic heme pathway), and Mito-H4 (amplified mitochondrial heme pathway) strains' heme concentrations were highest after 72 h of cultivation (Fig. 2). The background heme production of the parental D452-2 strain cultivated in YP50D medium was 1.5 ± 0.2 mg/L. The *S. cerevisiae* Cyto-H4 and Mito-H4 strains produced higher levels of heme than the control D452-2 strain; however, the magnitude of the increase in heme concentration by the Mito-H4 strain was greater than that by the Cyto-H4 strain. Moreover, the *S. cerevisiae* Mito-H4 strain showed a 3.0-fold increase in heme concentration compared with the D452-2 strain. This result indicated that the *S. cerevisiae* Mito-H4 strain produced heme efficiently because of the high expression levels of the four genes involved in heme biosynthesis and the mitochondrial compartmentalization of the four enzymes.

Effects of introducing the coproporphyrin-dependent pathway on *S. cerevisiae*'s heme production

In addition to optimizing the endogenous PPD pathway in *S. cerevisiae*, the non-canonical but thermodynamically favorable CPD pathway was introduced to enhance the production yield of heme. To this end, HemQs from *C. glutamicum* (HemQ^{Cg}) and *B. subtilis* (HemQ^{Bs}), both Gram-positive bacteria with GRAS status, were introduced into the *S. cerevisiae* Mito-H4 strain that contained the mitochondrial PPD pathway. The substrate for HemQ, copro-heme, was synthesized in the mitochondrial fraction of the *S. cerevisiae* Mito-H4 strain; therefore, HemQ was also relocalized to the mitochondria by attaching MTS9 to its N-terminus (Fig. 1B). As controls, HemQ^{Cg} and HemQ^{Bs} without MTS were introduced into the *S. cerevisiae* Mito-H4 strain. As a result, a set of the following four *S. cerevisiae* strains with the CPD pathway was constructed: H4+HemQ^{Cg}, the Mito-H4 strain expressing HemQ^{Cg} without MTS; H4+HemQ^{Bs}, the Mito-H4 strain expressing HemQ^{Bs} without MTS; H4+$_{MTS9}$HemQ^{Cg}, the Mito-H4 strain expressing HemQ^{Cg} with N-terminal MTS9; H4+$_{MTS9}$HemQ^{Bs}, the Mito-H4 strain expressing HemQ^{Bs} with N-terminal MTS9 (Table S1).

Before comparing the heme concentrations of the resulting *S. cerevisiae* strains, crude enzyme extract assays of HEM15 and HemQ were performed to confirm the functional expression of heterologous HemQ. The crude HEM15 enzymes present in cell lysates of the wild-type D452-2 strain and recombinant strains expressing HemQ in the cytoplasm (HemQ^{Cg} and HemQ^{Bs}) and mitochondria ($_{MTS9}$HemQ^{Cg} and $_{MTS9}$HemQ^{Bs}) were assayed with protoporphyrin IX (the substrate for HEM15), and showed that the amount of heme produced by each strain was not significantly different (Fig. 3A). In the CPD pathway, coproporphyrin III is converted to heme in two consecutive reactions catalyzed by HEM15 and HemQ (Fig. 1B). The in vitro HEM15 activity in the *S. cerevisiae* D452-2, HemQ^{Cg}, HemQ^{Bs}, $_{MTS9}$HemQ^{Cg}, and $_{MTS9}$HemQ^{Bs} strains were similar (Fig. 3A), suggesting the efficiency of heme synthesis from coproporphyrin III is dependent on HemQ activity. Although no enzymes predicted to have HemQ activity in *S. cerevisiae* have previously been identified, 1.3 ± 0.1 μM of heme was synthesized when a crude enzyme extract of the wild-type D452-2 was assayed with coproporphyrin III (Fig. 3B). This result indicates that an enzyme capable of converting copro-heme to heme is present in *S. cerevisiae*, possibly an unknown enzyme. Therefore, future research should focus on isolating and identifying this enzyme by performing affinity purification using copro-heme immobilized on a solid support and incubating it with the cell extract to separate it based on differences in its binding interaction. Notably, the introduction of cytoplasmic and mitochondrial HemQ increased in vitro HemQ activity, resulting in 2.6–3.9-fold higher heme synthesis efficiencies than the parental D452-2 strain (Fig. 3B). Among the four recombinant *S. cerevisiae* strains, the $_{MTS9}$HemQ^{Cg} strain expressing the mitochondrial HemQ^{Cg} showed the highest in vitro HemQ activity. The HemQ^{Cg} activity was higher in the mitochondria than in the cytoplasm, presumably because the environment for the folding of HemQ^{Cg} is more favorable in mitochondria compared with the cytoplasm. Previous studies have reported that mitochondria have lower oxygen concentration, higher pH, and a more reducing redox potential[23,24]. Currently, research is in progress to identify the key factors affecting HemQ^{Cg} activity in mitochondria.

Although cytoplasmic expression of HemQ increased HemQ activity in the *S. cerevisiae* HemQ^{Cg} and HemQ^{Bs} strains (Fig. 3B), cytoplasmic expression of HemQ was not expected to have a significant effect on heme production because the precursor of HemQ (i.e., copro-heme) is present in the mitochondria. In agreement with this reasoning, the maximum heme concentrations of the H4+HemQ^{Cg} and H4+HemQ^{Bs} strains were similar to that of the parental Mito-H4 strain (Fig. 4). However, the maximum heme concentrations of the H4+$_{MTS9}$HemQ^{Cg} and H4+$_{MTS9}$HemQ^{Bs} strains, which contained the mitochondrial HemQ, were 65% and 46% higher than the corresponding value for the Mito-H4 strain (Fig. 4). Because HemQ expression cassettes were introduced into *S. cerevisiae* using an episomal plasmid containing aureobasidin A as a selection marker, aureobasidin A was added to the culture medium in the fermentation experiments, including for the engineered strains expressing HemQ. The presence of aureobasidin A slightly extended the strains' lag phase, and the cultivation time required to achieve maximum heme concentration increased from 72 to 96 h; therefore, the heme concentrations were compared at the cultivation time of 96 h for further heme production experiments. Notably, the *S. cerevisiae* H4+$_{MTS9}$HemQ^{Cg} strain exhibited the highest in vitro HemQ activity (Fig. 3B) and maximum heme concentration (Fig. 4); consequently, the efficient production of heme in the H4+$_{MTS9}$HemQ^{Cg} strain was attributed to the functional expression of HemQ. These results suggest that the subcellular localization of HemQ in *S. cerevisiae* plays an important role in heme production via the CPD pathway.

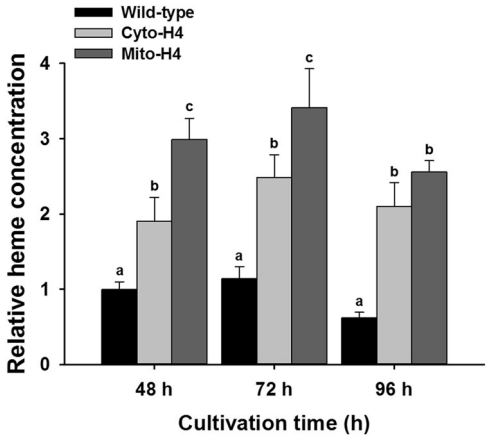

Fig. 2 | Heme concentrations in the wild-type *Saccharomyces cerevisiae* D452-2 and the engineered (Cyto-H4 and Mito-H4) strains after cultivation for 48, 72, and 96 h. The relative fold change was calculated based on the heme concentrations of the sample strains compared with those of the D452-2 strain after cultivation for 48 h. Results are the mean of three experiments, and error bars indicate standard deviations. Different letters represent significantly different means (Tukey honestly significant difference tests, $p < 0.05$). Cyto-H4, D452-2 *HIS3*::P_{GPD}-*HEM2*-T_{CYC1}, *LEU2*::P_{GPD}-*HEM3*-T_{CYC1}, *URA3*::P_{GPD}-*HEM12*-T_{CYC1}, and *CS6*::P_{GPD}-*HEM4*-T_{CYC1}; Mito-H4, D452-2 *HIS3*::$P_{GPD\text{-}MTS1}$*HEM2*-T_{CYC1}, *LEU2*::$P_{GPD\text{-}MTS4}$*HEM3*-T_{CYC1}, *URA3*::$P_{GPD\text{-}MTS12}$*HEM12*-T_{CYC1}, and *CS6*::$P_{GPD\text{-}MTS17}$*HEM4*-T_{CYC1}.

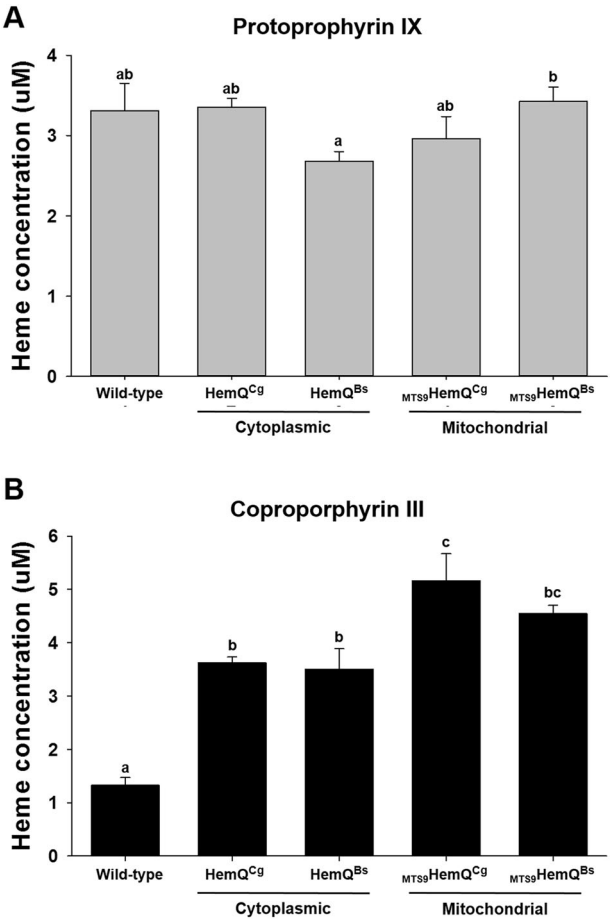

Fig. 3 | Effect of subcellular localization of HemQ on enzyme activity toward protoporphyrin IX and coproporphyrin III. Relative enzymatic activity of the crude enzyme extracts of the wild-type *Saccharomyces cerevisiae* D452-2 and the engineered strains with the cytoplasmic ($HemQ^{Cg}$ and $HemQ^{Bs}$) or mitochondrial ($_{MTS9}HemQ^{Cg}$ and $_{MTS9}HemQ^{Bs}$) HemQ on protoporphyrin IX (**A**) and coproporphyrin III (**B**). Results are the mean of three experiments, and error bars indicate standard deviations. Different letters represent significantly different means (Tukey honestly significant difference tests, $p < 0.05$). $HemQ^{Cg}$, D452-2 harboring $pHemQ^{Cg}$; $HemQ^{Bs}$, D452-2 harboring $pHemQ^{Bs}$; $_{MTS9}HemQ^{Cg}$, D452-2 harboring $p_{MTS9}HemQ^{Cg}$; $_{MTS9}HemQ^{Bs}$, D452-2 harboring $p_{MTS9}HemQ^{Bs}$.

Enhanced heme production via the introduction of *E. coli* Group-I HSP60 chaperonins (GroEL and GroES)

The functional expression levels of several bacterial enzymes expressed in *S. cerevisiae* have previously been shown to be significantly enhanced by co-expressing *E. coli* Group-I HSP60 chaperonins (GroEL and GroEL)[25,26]; this is likely because the cytoplasmic HSP60 chaperonins present in *S. cerevisiae* are structurally and functionally different from the GroEL/ES chaperonins[25,27]. To this end, the *groLS* genes coding for GroEL and GroES were co-expressed with $_{MTS9}HemQ^{Cg}$ in the *S. cerevisiae* $_{MTS9}HemQ^{Bs}$+GroELS strain to enhance the functional expression level of $HemQ^{Cg}$. In addition, the *S. cerevisiae* D452-2 strain (GroELS) containing GroEL and GroES without HemQ was constructed as a control. Protoporphyrin IX is converted to heme in the one-step reaction catalyzed by HEM15, whereas coproporphyrin III is converted to heme in two consecutive reactions catalyzed by HEM15 and HemQ (Fig. 1B). Unexpectedly, the expression of the GroEL/ES chaperonins, even in the absence of HemQ, improved the in vitro conversion efficiency of protoporphyrin IX and coproporphyrin III (Fig. 5). This result indicated that the additional HSP60 chaperonins, distinct from the native HSP60 chaperonins, supported proper folding of various endogenous enzymes present in *S. cerevisiae*, including HEM15 and unknown enzymes possessing HemQ activity. Accordingly, the GroEL/ES chaperonin co-expression strategy may increase the production of a variety of target compounds, not just heme. In line with this expectation, the magnitude of the increased activity of crude HemQ (heterologous enzyme) in the $_{MTS9}HemQ^{Cg}$+GroELS strain via the introduction of the GroEL/ES chaperonins was found to be greater than the activity of crude HEM15 (endogenous enzyme). As a result, the *S. cerevisiae* $_{MTS9}HemQ^{Bs}$+GroELS strain showed a 1.2- and 2.6-fold increase in heme synthesis from protoporphyrin IX and coproporphyrin III, respectively, compared with the background $_{MTS9}HemQ^{Bs}$ strain lacking GroEL/ES chaperonins.

To investigate if the increased activity of HEM15 and HemQ via the introduction of GroEL/ES chaperonins enhanced heme production, batch fermentation was performed using *S. cerevisiae* wild-type D452-2, GroELS (D452-2 strain expressing GroEL and GroES), Mito-H4 (D452-2 strain containing the mitochondrial PPD pathway), H4+$_{MTS9}HemQ^{Cg}$ (Mito-H4 strain expressing mitochondrial $HemQ^{Cg}$), and H4+$_{MTS9}HemQ^{Cg}$+GroELS (Mito-H4 strain expressing mitochondrial $HemQ^{Cg}$, GroEL, and GroES) strains, and their heme production was compared after 96 h of cultivation. Surprisingly, the introduction of GroEL and GroES into the wild-type *S. cerevisiae* D452-2 strain resulted in a 2.2-fold increase in heme production (Fig. 6). This result is likely due to the increase in overall functional expression levels of enzymes involved in heme biosynthesis, including HEM15 (Fig. 5A). Consistent with the in vitro enzyme activity results (Fig. 5), the introduction of GroEL and GroES into the *S. cerevisiae* H4+$_{MTS9}HemQ^{Cg}$ strain increased the heme concentration by 17%, resulting in the production of 4.6 mg/L of heme with a yield of 0.1 mg of heme/g of glucose in the H4+$_{MTS9}HemQ^{Cg}$+GroELS strain.

It is presently unclear if HEM13 resides in the cytosolic or mitochondrial fraction; therefore, HEM13 with and without the N-terminal MTS (for mitochondrial and cytoplasmic expression, respectively) was further overexpressed in the *S. cerevisiae* Mito-H4 strain. However, all *S. cerevisiae* strains exhibited similar heme production concentrations (Supplementary Fig. 2), indicating that HEM13 activity in the mitochondrial fraction of the Mito-H4 strain is not a rate-limiting factor for heme biosynthesis.

A recent study by Guo et al.[12] showed that the fed-batch fermentation of an engineered *S. cerevisiae* with an optimized heme biosynthetic pathway and increased tolerance to heme toxicity produced 380.5 mg/L of heme, the

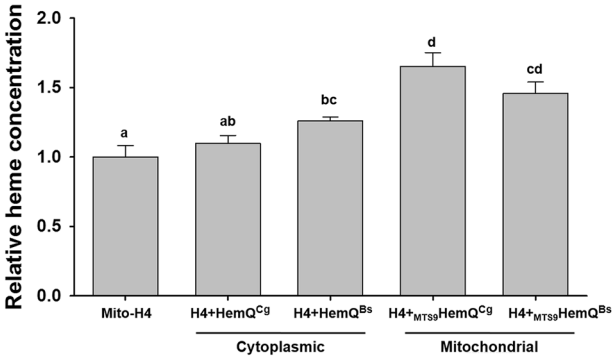

Fig. 4 | Heme concentrations in the *Saccharomyces cerevisiae* Mito-H4 and Mito-H4 strains with the cytoplasmic (HemQ^{Cg} and HemQ^{Bs}) or mitochondrial ($_{MTS9}$HemQ^{Cg} and $_{MTS9}$HemQ^{Bs}) HemQ after cultivation for 96 h. The relative fold change was calculated based on the heme concentrations of the sample strains compared with the Mito-H4 strain. Results are the mean of three experiments, and error bars indicate the standard deviation. Different letters represent significantly different means (Tukey honestly significant difference tests, $p < 0.05$). Mito-H4, D452-2 *HIS3*::$P_{GPD\text{-}MTS1}$*HEM2*-T_{CYC1}, *LEU2*::$P_{GPD\text{-}MTS4}$*HEM3*-T_{CYC1}, *URA3*::$P_{GPD\text{-}MTS12}$*HEM12*-T_{CYC1}, and *CS6*::$P_{GPD\text{-}MTS17}$*HEM4*-T_{CYC1}; H4+HemQ^{Cg}, Mito-H4 harboring pHemQ^{Cg}; H4+HemQ^{Bs}, Mito-H4 harboring pHemQ^{Bs}; H4+$_{MTS9}$HemQ^{Cg}, Mito-H4 harboring p$_{MTS9}$HemQ^{Cg}; H4+$_{MTS9}$HemQ^{Bs}, Mito-H4 harboring p$_{MTS9}$HemQ^{Bs}.

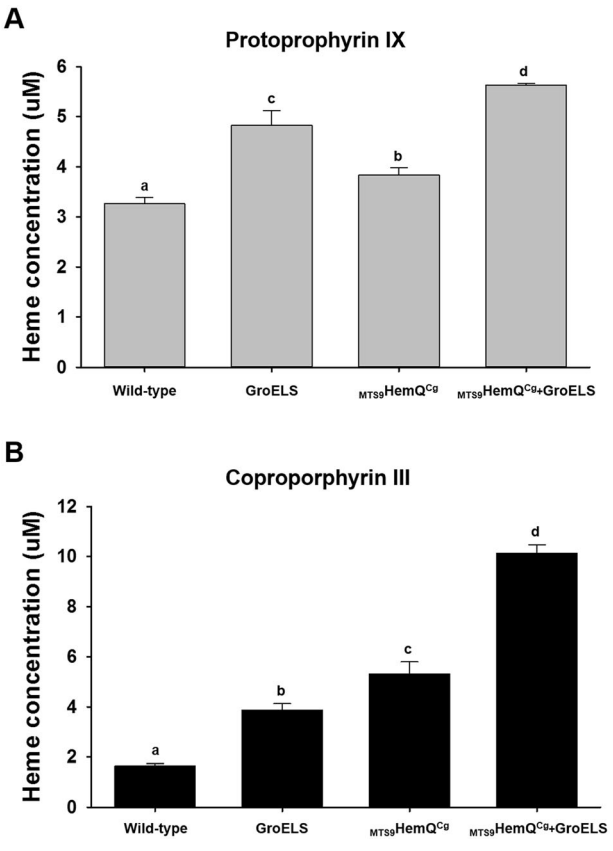

Fig. 5 | Effect of strain engineering on enzyme activity toward protoporphyrin IX and coproporphyrin III. Relative enzymatic activity of the crude enzyme extracts of the wild-type *Saccharomyces cerevisiae* D452-2 and engineered strains on protoporphyrin IX (**A**) and coproporphyrin III (**B**). Results are the mean of three experiments, and error bars indicate the standard deviation. Different letters represent significantly different means (Tukey honestly significant difference tests, $p < 0.05$). GroELS, D452-2 *URA3*::P_{tHXT7}-*groES*-T_{CYC1} and *CS8*::P_{GPD}-*groEL*-T_{CYC1}; $_{MTS9}$HemQ^{Cg}, D452-2 harboring p$_{MTS9}$HemQ^{Cg}; $_{MTS9}$HemQ^{Cg}+GroELS, GroELS harboring p$_{MTS9}$HemQ^{Cg}.

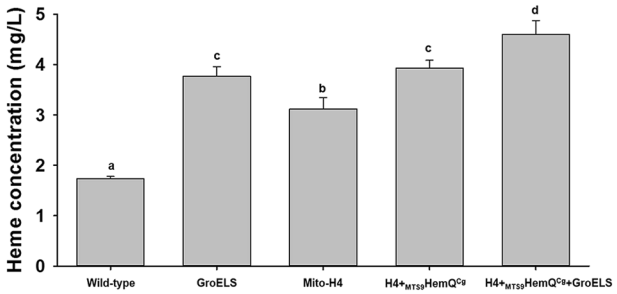

Fig. 6 | Comparison of heme production by the wild-type *Saccharomyces cerevisiae* D452-2 and engineered strains after cultivation for 96 h. Results are the mean of three experiments, and error bars indicate the standard deviation. Different letters represent significantly different means (Tukey honestly significant difference tests, $p < 0.05$). GroELS, D452-2 *URA3*::P_{tHXT7}-*groES*-T_{CYC1} and *CS8*::P_{GPD}-*groEL*-T_{CYC1}; Mito-H4, D452-2 *HIS3*::$P_{GPD\text{-}MTS1}$*HEM2*-T_{CYC1}, *LEU2*::$P_{GPD\text{-}MTS4}$*HEM3*-T_{CYC1}, *URA3*::$P_{GPD\text{-}MTS12}$*HEM12*-T_{CYC1}, and *CS6*::$P_{GPD\text{-}MTS17}$*HEM4*-T_{CYC1}; H4+$_{MTS9}$HemQ^{Cg}, Mito-H4 harboring p$_{MTS9}$HemQ^{Cg}; $_{MTS9}$HemQ^{Cg}+GroELS, GroELS harboring p$_{MTS9}$HemQ^{Cg}.

highest concentration of yeast-based heme production reported to date. In the previous study, an adaptive evolution strategy combined with a CRISPR-assisted genome-scale random mutagenesis was used to enhance resistance to heme toxicity. After five rounds of evolutionary screening, a mutant with a 7.3-fold increase in heme production was isolated based on its red color[12]. Since an engineered *S. cerevisiae* strain with only the heme biosynthetic pathway optimized (without increased heme tolerance) produced 5.9 mg/L of heme with a yield of 0.3 mg of heme/g of glucose in batch fermentation[12], future studies using a similar laboratory evolution for improving cellular tolerance to heme are required to maximize the heme production efficiency of the H4+$_{MTS9}$HemQ^{Cg}+GroELS strain constructed in this study. Furthermore, the extracellular secretion of heme-binding proteins, such as leghemoglobin, is expected to improve the strain's heme production yield and concentration by reducing its intracellular heme concentration, thereby alleviating heme toxicity.

In this study, we demonstrated that compartmentalization of the PPD pathway into the mitochondria increased heme production in *S. cerevisiae* 3.0-fold, whereas overexpression of the same pathway in the cytoplasm only improved yields 2.2-fold. Adding the heterologous CPD pathway to the mitochondrial fraction of the *S. cerevisiae* Mito-H4 strain, which contained the mitochondrial PPD pathway, resulted in a 65% increase in heme production compared with the background strain. Furthermore, enhancing the functional expression level of the key enzyme (i.e., HemQ^{Cg}) in the CPD pathway through the co-expression of *E. coli* Group-I HSP60 chaperonins led to a significant increase in *S. cerevisiae*'s heme synthesis activity in vitro and in vivo. As a result, the *S. cerevisiae* H4+$_{MTS9}$HemQ^{Cg}+GroELS strain, which contained the mitochondrial PPD and CPD pathways and the Group-I HSP60 chaperonins, produced 4.6 mg/L of heme, which was 17% higher than the H4+$_{MTS9}$HemQ^{Cg} strain without Group-I HSP60 chaperonins.

Methods

Strains and plasmids

The *E. coli* TOP10 (Invitrogen, Carlsbad, CA, USA) and *S. cerevisiae* D452-2[28] strains were used for gene cloning and heme production, respectively. The *S. cerevisiae* strains and plasmids used in this study are listed in Table S1.

Genetic manipulation

The codon-optimized genes coding for HemQ from *C. glutamicum* and *B. subtilis* were synthesized by Bionics Co., Ltd. (Seoul, Republic of Korea). Table S2 lists the primer sets used for the amplification of the genes coding the heme biosynthesis enzymes, and the iron-coproporphyrin (coproheme) decarboxylases (HemQs) and construction of their expression cassettes. The resulting polymerase chain reaction products were combined

using NEBuilder HiFi DNA Assembly Master Mix (New England Biolabs, Ipswich, MA, USA) as specified by the manufacturer.

Integrative plasmids containing the genes coding for enzymes involved in heme biosynthesis and episomal plasmids containing the genes coding for the HemQs were transformed into *S. cerevisiae* D452-2 using a yeast EZ-transformation kit (BIO101, Vista, CA, USA). Transformants were isolated on solid yeast synthetic complete medium (6.7 g/L yeast nitrogen base and 20 g/L glucose) containing 40 g/L of agar with the appropriate amino acids and nucleotides. In addition, 200 μg/mL of geneticin (G418) and 0.15 μg/mL of aureobasidin A were added as selection pressure as required.

The GroEL (GPDp-GroEL-CYC1t) and $_{MTS12}$HEM12 (GPDp-$_{MTS12}$HEM12-CYC1t) expression cassettes were introduced into the CS8[29] and CS11 loci, respectively, using the genome editing system based on clustered regularly interspaced palindromic repeats (CRISPR)/CRISPR-associated protein 9 (Cas9) as previously described[30]. In *S. cerevisiae*, the CS8 locus is an intergenic region located on chromosome XVI between *YPR015C* and *YPR014C*, and the CS11 locus is the intergenic region between *AAP1* and *YHK8*. Briefly, guide ribonucleic acid (gRNA) plasmids and repaired deoxyribonucleic acid (DNA) fragments, amplified with primers listed in Table S2, were co-transformed into *S. cerevisiae* strains containing pCas9_AUR to construct the H4+$_{MTS9}$HemQ^{Cg}+GroELS strain (Table S1).

Media and culture conditions

The *E. coli* was grown in Luria–Bertani medium (10 g/L tryptone, 5 g/L yeast extract, and 10 g/L NaCl) containing 50 μg/mL of ampicillin for gene cloning. The *S. cerevisiae* strains without the HemQ expression cassette were pre-cultured at 25 °C and 250 rpm for 48 h in yeast synthetic complete medium (6.8 g/L yeast nitrogen base, 1.66 g/L synthetic complete supplement without histidine, leucine, and uracil, and 20 g/L glucose) containing 200 μg/mL of G418. Yeast synthetic complete medium containing 200 μg/mL of G418 and 0.15 μg/mL of aureobasidin A was used for pre-cultivation of the *S. cerevisiae* strains harboring the episomal plasmid with the HemQ expression cassette. The pre-cultured cells were harvested and inoculated into the main cultures with an initial optical density of 1.0 at 600 nm. The main fermentation experiments were carried out for 96 h in a baffled flask containing 100 mL of YP50D medium (10 g/L yeast extract, 20 g/L Bacto™ Peptone, and 50 g/L glucose). The *S. cerevisiae* strains with and without the HemQ expression cassette were cultivated in YP50D medium with and without 0.15 μg/mL of aureobasidin A, respectively. The temperature and agitation speed were maintained at 25 °C and 250 rpm throughout the fermentation.

Mitochondrial protein preparation and analysis of *HEM2* gene expression

The yeast mitochondrial protein fraction was isolated using a Minute™ yeast mitochondria enrichment kit (Invent Biotechnologies, Inc., Plymouth, MN, USA) according to the manufacturer's instructions. To visualize the aminolevulinate dehydratase (HEM2) protein, the mitochondrial protein samples fractionated by 12% (w/v) sodium dodecyl sulfate-polyacrylamide gel electrophoresis were transferred to polyvinylidene difluoride membranes (Millipore®, Merck KGaA, Darmstadt, Germany). For the immunoblot assays, HEM2 with a C-terminal Myc proto-oncogene protein tag was detected using an anti-Myc antibody (sc-42, 1:1000 dilution), as specified by the manufacturer (Santa Cruz Biotechnology, Inc., Dallas, TX, USA).

Analytical methods

A spectrophotometer (OPTIZEN POP, Mecasys Co., Ltd., Yuseong-gu, Daejeon, Republic of Korea) was used to measure cell growth at an optical density measured at 600 nm (OD_{600}). Concentrations of glucose, glycerol, acetic acid, and ethanol were determined using a high-performance liquid chromatography (HPLC) system (Ultimate 3000; Thermo Fisher Scientific Inc., Waltham, MA, USA) equipped with a Rezex ROA-organic acid H^+ column (Phenomenex, Torrance, CA, USA). Metabolites were separated at an isocratic temperature of 60 °C at a flow rate of 0.6 mL/min in 0.01 N sulfuric acid (H_2SO_4) and then passed through a reflective index detector.

To determine intracellular heme concentration, the culture broth was centrifuged at 15,000 rpm for 10 min. The cells were harvested at OD_{600} × mL of culture = 60 (i.e., if the OD_{600} value was 30, 2.0 mL of culture was harvested). The harvested cells were resuspended in 0.4 mL of Y-PER™ (Thermo Fisher Scientific Inc., Waltham, MA, USA) and lysed according to the manufacturer's instructions. After adding 1.2 mL of acetonitrile to the cell lysate, the mixture was incubated for 5 min at room temperature with occasional shaking. The precipitates were collected by centrifugation at 4000 rpm for 5 min and then reacted with 1.6 mL of a mixture containing acetonitrile and 1.7 M hydrochloric acid (HCl) at a volume ratio of 8:2 at 25 °C and 250 rpm for 20 min. For neutralization, 0.4 mL of saturated magnesium sulfate ($MgSO_4$) solution containing 100 μg/L of sodium chloride (NaCl) was added to 1.6 mL of the reaction mixture. The reaction mixture was incubated at 25 °C and 250 rpm for 20 min and then centrifuged at 4000 rpm for 5 min, and an acetonitrile layer was filtered (0.2 μm) before conducting the HPLC analysis. The heme concentration was measured using a Thermo Fisher Ultimate 3000 HPLC equipped with a YMC-Pack ODS-A column (YMC Co., Ltd., Kyoto, Japan). The heme was separated at a constant temperature of 50 °C with mobile phase A and mobile phase B in a gradient mode (0 min, A:B = 80:20; 10–11.1 min, A:B = 0:100; 12–25 min, A:B = 80:20 [% v/v]) at a flow rate of 0.4 mL/min and then passed through an ultraviolet detector (400 nm). Mobile phase A was a mixture of acetonitrile and water (5:95 [% v/v]) containing 1.2 g/L of formic acid, whereas mobile phase B was a mixture of acetonitrile and water (95:5 [% v/v]) containing 1.2 g/L of formic acid.

Enzyme activity assays

To prepare crude enzyme extract, *S. cerevisiae* cells grown at 30 °C and 250 rpm for 72 h in YP50D medium containing 0.15 μg/mL of aureobasidin A were lysed using glass beads (I.D. 0.5 mm, BioSpec Products, Bartlesville, OK, USA), as specified by the manufacturer. Protein concentrations were determined using a protein assay kit (Bio-Rad Laboratories, Inc., Hercules, CA, USA) using bovine serum albumin as the standard. The reaction mixture for the HEM15 and/or HemQ activities was composed of 66 mM Tris-HCl (pH 8.0) containing 3.3% of Tween 20, 5 mM of glutathione, 100 μM of ferrous ammonium sulfate, 100 μM of β-mercaptoethanol, and 0.6 mg/mL of crude enzyme extract; 25 μM of protoporphyrin IX or coproporphyrin III was added to the reaction mixture and incubated at 30 °C for 16 or 8 h, respectively. The heme concentration in the reaction mixture was measured using the HPLC system as described previously.

Statistical analysis

Statistical analyses were performed using SPSS Statistics software (v.28.0, IBM Corp., Armonk, NY, USA). All data are presented as the mean ± standard deviation. One-way analysis of variance was performed, and statistical significance was assessed using Tukey's Honestly Significant Difference (HSD) tests, with the significance level set at $p < 0.05$.

Data availability

Data available upon request to the corresponding author.

Received: 14 November 2024; Accepted: 12 May 2025;
Published online: 22 May 2025

References

1. Gallio, A. E., Fung, S. S., Cammack-Najera, A., Hudson, A. J. & Raven, E. L. Understanding the logistics for the distribution of heme in cells. *JACS Au* **1**, 1541–1555 (2021).
2. He, L. et al. Antioxidants maintain cellular redox homeostasis by elimination of reactive oxygen species. *Cell. Physiol. Biochem.* **44**, 532–553 (2017).

3. Chiabrando, D., Vinchi, F., Fiorito, V., Mercurio, S. & Tolosano, E. Heme in pathophysiology: a matter of scavenging, metabolism and trafficking across cell membranes. *Front. Pharmacol.* **5**, 61 (2014).
4. Anderson, K. E. & Collins, S. D. Open-label study of hemin for acute porphyria: clinical practice implications. *Am. J. Med.* **119**, e19–e24 (2006).
5. Simsa, R. et al. Extracellular heme proteins influence bovine myosatellite cell proliferation and the color of cell-based meat. *Foods* **8**, 521 (2019).
6. Yarra, P., Faust, D., Bennett, M., Rudnick, S. & Bonkovsky, H. L. Benefits of prophylactic heme therapy in severe acute intermittent porphyria. *Mol. Genet. Metab. Rep.* **19**, 100450 (2019).
7. Ryu, W. H. et al. Heme biomolecule as redox mediator and oxygen shuttle for efficient charging of lithium-oxygen batteries. *Nat. Commun.* **7**, 12925 (2016).
8. Waltz, E. Appetite grows for biotech foods with health benefits. *Nat. Biotechnol.* **37**, 573–580 (2019).
9. Zhao, X., Zhou, J., Du, G. & Chen, J. Recent advances in the microbial synthesis of hemoglobin. *Trends Biotechnol.* **39**, 286–297 (2021).
10. Choi, K. R., Yu, H. E., Lee, H. & Lee, S. Y. Improved production of heme using metabolically engineered *Escherichia coli*. *Biotechnol. Bioeng.* **119**, 3178–3193 (2022).
11. Rietschel, E. T. et al. Bacterial endotoxin: chemical constitution, biological recognition, host response, and immunological detoxification. *Curr. Top. Microbiol. Immunol.* **216**, 39–81 (1996).
12. Guo, Q. et al. Multidimensional engineering of *Saccharomyces cerevisiae* for the efficient production of heme by exploring the cytotoxicity and tolerance of heme. *Metab. Eng.* **85**, 46–60 (2024).
13. Tao, Z. et al. Yeast extract: characteristics, production, applications and future perspectives. *J. Microbiol. Biotechnol.* **33**, 151–166 (2023).
14. Zhang, J., Kang, Z., Chen, J. & Du, G. Optimization of the heme biosynthesis pathway for the production of 5-aminolevulinic acid in *Escherichia coli*. *Sci. Rep.* **5**, 8584 (2015).
15. Xue, J. et al. Systematic engineering of *Saccharomyces cerevisiae* for efficient synthesis of hemoglobins and myoglobins. *Bioresour. Technol.* **370**, 128556 (2023).
16. Yu, F. et al. Biosynthesis of high-active hemoproteins by the efficient heme-supply *Pichia pastoris* chassis. *Adv. Sci.* **10**, e2302826 (2023).
17. Liu, L., Martinez, J. L., Liu, Z., Petranovic, D. & Nielsen, J. Balanced globin protein expression and heme biosynthesis improve production of human hemoglobin in *Saccharomyces cerevisiae*. *Metab. Eng.* **21**, 9–16 (2014).
18. Medlock, A. E. et al. Identification of the mitochondrial heme metabolism complex. *PLoS ONE* **10**, e0135896 (2015).
19. Dailey, H. A., Gerdes, S., Dailey, T. A., Burch, J. S. & Phillips, J. D. Noncanonical coproporphyrin-dependent bacterial heme biosynthesis pathway that does not use protoporphyrin. *Proc. Natl Acad. Sci. USA* **112**, 2210–2215 (2015).
20. Beas, J. Z., Videira, M. A. M. & Saraiva, L. M. Regulation of bacterial haem biosynthesis. *Coord. Chem. Rev.* **452**, 214286 (2022).
21. Seok, J., Ko, Y. J., Lee, M. E., Hyeon, J. E. & Han, S. O. Systems metabolic engineering of *Corynebacterium glutamicum* for the bioproduction of biliverdin via protoporphyrin independent pathway. *J. Biol. Eng.* **13**, 28 (2019).
22. Dong, C. et al. Cloning and characterization of a panel of mitochondrial targeting sequences for compartmentalization engineering in *Saccharomyces cerevisiae*. *Biotechnol. Bioeng.* **118**, 4269–4277 (2021).
23. Mori, M. P. et al. Mitochondrial respiration reduces exposure of the nucleus to oxygen. *J. Biol. Chem.* **299**, 103018 (2023).
24. Starkov, A. A. The role of mitochondria in reactive oxygen species metabolism and signaling. *Ann. N. Y. Acad. Sci.* **1147**, 37–52 (2008).
25. Xia, P. F. et al. GroE chaperonins assisted functional expression of bacterial enzymes in *Saccharomyces cerevisiae*. *Biotechnol. Bioeng.* **113**, 2149–2155 (2016).
26. Jeon, G. B. et al. Efficient production of glutathione in *Saccharomyces cerevisiae* via a synthetic isozyme system. *Biotechnol. J.* **18**, e2200398 (2023).
27. Temer, B. et al. Conversion of an inactive xylose isomerase into a functional enzyme by co-expression of GroEL-GroES chaperonins in *Saccharomyces cerevisiae*. *BMC Biotechnol.* **17**, 71 (2017).
28. Hosaka, K., Nikawa, J., Kodaki, T. & Yamashita, S. A dominant mutation that alters the regulation of *INO1* expression in *Saccharomyces cerevisiae*. *J. Biochem.* **111**, 352–358 (1992).
29. Kwak, S. et al. Enhanced isoprenoid production from xylose by engineered *Saccharomyces cerevisiae*. *Biotechnol. Bioeng.* **114**, 2581–2591 (2017).
30. Lee, Y. G., Jin, Y. S., Cha, Y. L. & Seo, J. H. Bioethanol production from cellulosic hydrolysates by engineered industrial *Saccharomyces cerevisiae*. *Bioresour. Technol.* **228**, 355–361 (2017).

Acknowledgements

This study was financially supported by the National Research Foundation of Korea Grant (2022R1C1C1003154 and RS-2024-00440975), funded by the Korean Ministry of Science, ICT, and Future Planning. This research was also supported by the Chung-Ang University Graduate Research Scholarship in 2023.

Author contributions

J.Y.W.: Methodology, Investigation. H.L.: Investigation, Visualization. E.B.Y.: Formal analysis. Y.C.: Conceptualization, Writing – review & editing. S.K.: Conceptualization, Supervision, Writing - original draft preparation.

Competing interests

The authors declare that they have no conflicts of interest.

Additional information

Supplementary information The online version contains supplementary material available at https://doi.org/10.1038/s41538-025-00453-4.

Correspondence and requests for materials should be addressed to Young-Wook Chin or Sun-Ki Kim.

Reprints and permissions information is available at http://www.nature.com/reprints

Publisher's note Springer Nature remains neutral with regard to jurisdictional claims in published maps and institutional affiliations.

Open Access This article is licensed under a Creative Commons Attribution-NonCommercial-NoDerivatives 4.0 International License, which permits any non-commercial use, sharing, distribution and reproduction in any medium or format, as long as you give appropriate credit to the original author(s) and the source, provide a link to the Creative Commons licence, and indicate if you modified the licensed material. You do not have permission under this licence to share adapted material derived from this article or parts of it. The images or other third party material in this article are included in the article's Creative Commons licence, unless indicated otherwise in a credit line to the material. If material is not included in the article's Creative Commons licence and your intended use is not permitted by statutory regulation or exceeds the permitted use, you will need to obtain permission directly from the copyright holder. To view a copy of this licence, visit http://creativecommons.org/licenses/by-nc-nd/4.0/.

© The Author(s) 2025